INDIAN JOURNAL OF SCIENCE AND TECHNOLOGY

ORIGINAL ARTICLE

Synthesis and Characterization of PPy-Fe(ClO_4)$_2$-Ag Nano-Composite and Their Study in H_2S Gas Sensor at Room Temperature

Raju P Tandel [1]*, Minal P Patil[2], Vinod S More[2], Gitesh G Padhye[3], Tatyarao N Ghorude[2]

1 Sonopant Dandekar College, Palghar, Maharashtra, India
2 N B Mehta Science College, Bordi, Dahanu, Maharashtra, India
3 Thakur College of Science and Commerce, Kandivali, Mumbai, India

OPEN ACCESS

Received: 25/01/2025
Accepted: 17/05/2025
Published: 30/05/2025

Citation: Tandel RP, Patil MP, More VS, Padhye GG, Ghorude TN (2025) Synthesis and Characterization of PPy-Fe(ClO_4)$_2$-Ag Nano-Composite and Their Study in H_2S Gas Sensor at Room Temperature. Indian Journal of Science and Technology 18(20): 1610-1622. https://doi.org/10.17485/IJST/v18i20.166

* **Corresponding author**.

rajutandel92@gmail.com

Funding: None

Competing Interests: None

Published By Indian Society for Education and Environment (iSee)

ISSN
Print: 0974-6846
Electronic: 0974-5645

Abstract

Objectives: The study aimed to synthesize and characterize a polypyrrole (PPy) nanocomposite doped with iron perchlorate [Fe(ClO_4)$_2$] and silver nanoparticles (Ag-NPs) for potential application as a room-temperature gas sensor, specifically targeting hydrogen sulfide (H_2S) gas detection. **Methods:** The PPy nanocomposite was synthesized through in situ chemical polymerization using ferric chloride ($FeCl_3$) as the oxidant, with a monomer-to-oxidant ratio of 1:1. Silver nanoparticles were prepared using the Turkevich method and incorporated as dopants. The structural, morphological, and chemical properties of the synthesized nanocomposite were analyzed using SEM, TEM, UV-Vis, FTIR and XRD techniques. Electrical conductivity was measured using a two-probe technique, and the material's gas-sensing performance was evaluated by exposing it to H_2S gas. **Findings:** The synthesized PPy-Fe(ClO_4)$_2$-Ag nanocomposite demonstrated excellent sensitivity to H_2S gas at room temperature. A sharp increase in current was observed upon exposure to H_2S gas, which quickly reverted when the gas was removed. The characterization results confirmed the successful incorporation of Ag nanoparticles and Fe(ClO_4)$_2$ into the PPy matrix, contributing to its enhanced electrical and sensing properties. **Novelty:** This study highlights the innovative use of a PPy-based nanocomposite doped with iron perchlorate and silver nanoparticles for highly sensitive and reversible H_2S gas detection at room temperature. The combination of these dopants enhances the material's electrical conductivity and sensing capabilities, offering a promising candidate for low-cost, efficient gas sensor applications.

Keywords: Polypyrrole; Silver nanoparticles; Iron per Chlorate; H_2S; Gas sensor

1 Introduction

Polypyrrole (PPy), a conducting polymer synthesized from the pyrrole monomer, its superior electrical conductivity, enhanced stability, mechanical properties, and ease of preparation have made it one of the most extensively studied conducting polymers[1]. PPy has found applications in diverse fields, including electrochromic devices, biosensors, micro actuators, anti-electrostatic coatings, polymeric batteries, optical switching devices, functional electrodes, and electronic components. Generally, PPy is an amorphous, black powder material composed of acid and peroxide. Its conductivity can be significantly enhanced through doping with electron-accepting halogens, and common chemical oxidants such as aqueous or anhydrous $FeCl_3$, iron (III), or copper (II) salts are often employed for this purpose[2].

Among various conducting polymers, including polyaniline (PANI)[3], polythiophene (PTh)[4], and polypyrrole (PPy)[5], PPy stands out due to its excellent electrical conductivity, environmental resilience, low toxicity, and versatility in gas-sensing applications. It has demonstrated the ability to detect gases such as nitrogen dioxide, ammonia, and hydrogen sulfide (H_2S).

Numerous PPy-based composites have been explored as room-temperature gas sensors for a wide range of gases, including PPy/Ag[6], PPy/ZnO and PPy/WO_3[7]. These composites exhibit remarkable sensitivity, selectivity, and response times. Sood et al. synthesized polypyrrole (PPy) using ammonium peroxydisulfate (APS) and ferric chloride ($FeCl_3$) as oxidants, reporting that PPy prepared with $FeCl_3$ demonstrated superior conductivity (2.22×10^{-4}S/cm) and enhanced thermal stability compared to APS-based PPy. In another study, Pagar et al. utilized a chemical synthesis method to fabricate PPy, characterizing the material through SEM, XRD, FTIR, and UV-visible spectroscopy at varying molar ratios[8]. Similarly, Dave et al. synthesized PPy using ferric chloride as an oxidant, varying the oxidant-to-monomer ratios, and observed conductivities ranging from 545.19 μS/cm to 215.78 μS/cm for the samples[9].

Metal oxide-based sensors, while highly sensitive and cost-effective, typically operate at elevated temperatures (200–500 °C), leading to high power consumption and limiting their practical applications[10]. Consequently, there has been significant interest in developing ambient-temperature gas sensors. Compared to pure PPy, PPy-Ag nanocomposites exhibit superior catalytic and optoelectronic sensing performance. This has motivated researchers to explore the development of PPy-Ag nanocomposites further[11]. Silver nanoparticles are known for their remarkable stability and compatibility with conducting oxides at both room and elevated temperatures. Moreover, they facilitate the formation of good ohmic contacts in polymer-metal oxide materials. PPy/Ag composites have been successfully employed as gas sensors for detecting H_2S[12], NO_2[13], and NH_3[14].

The growing industrial activities worldwide have led to increased emissions of hazardous gases such as H_2S, NH_3, CO, NO_2, Cl_2, CO_2, and various organic vapors, contributing significantly to environmental pollution. Hydrogen sulfide (H_2S), a toxic gas commonly encountered in industrial settings, poses severe health risks, including eye irritation, respiratory issues, nausea, and even death at high concentrations (>250 ppm). Therefore, the development of efficient gas sensors capable of rapidly detecting low concentrations of H_2S is critical to mitigating environmental pollution and ensuring public safety.

Herein, we report the successful synthesis of a PPy-$Fe(ClO_4)_2$-Ag nanocomposite via chemical polymerization of pyrrole in the presence of Ag nanoparticles (Ag NPs). The AgNPs were prepared using the Turkevich method and characterized using various techniques such as SEM, TEM, XRD, FTIR and UV-visible spectroscopy. Its electrical conductivity was evaluated using the two-probe technique. Furthermore, the nanocomposite's sensing capabilities for H_2S detection at room temperature were investigated, and the results are discussed in detail.

2 Methodology

2.1 Materials

Pyrrole (C_4H_5N) was acquired from Spectrochem Pvt. Ltd. in Mumbai and stored at a low temperature in a dark bottle. Before being used, this was double-distilled and kept in the refrigerator. Merck Ltd. in Mumbai provided the trisodium citrate ($Na_3C_6H_5O_7$), silver nitrate ($AgNO_3$), ferric chloride ($FeCl_3$), and iron per chlorate [$Fe(ClO_4)_2$]. These chemicals were used as received and were of AR grade. Double distilled water was utilized to prepare all of the solutions.

2.2 Methods

2.2.1. ***Synthesis of Silver nanoparticles (Ag NPs):***

For the production of silver nanoparticles (Ag NPs), the Turkevich method was introduced[15]. A standard experiment involved heating 50 ml of 1 mM $AgNO_3$ to boiling point. Dropwise additions of 5 ml of 10 mM trisodium citrate at a rate of about one drop every second. The solutions were vigorously mixed throughout this process, along with boiling temperature was

maintained as well. As Ag NPs formed, the solution's color gradually changed from colorless to golden yellow. The following is an expression of the reaction mechanism of Ag NPs creation (as suggested in Dong et al.)[15].

$$4Ag^{+} + Na_3C_6H_5O_7 + 2H_2O \xrightarrow{Heat} 4Ag^{0} + C_6H_5O_7H_3 + 3Na^{+} + H^{+} + O_2 \uparrow$$

2.2.2. *Synthesis of PPy . $Fe(ClO_4)_2$. Ag nanocomposite:*

The In situ chemical oxidation polymerization method was used to create the PPy-Ag nanocomposite[16]. In a typical synthesis experiment, 35 millilitres of Ag NPs solution was placed in the ice bath (0° to 5°C) and agitated with a magnetic stirrer for 30 minutes before 1 milliliter of pyrrole was added dropwise. The mixture stirred until all of the pyrrole had been dissolved. After cooling, the $FeCl_3$ (1M) aqueous solution was added dropwise in the solution above. After turning from golden yellow to grey, the solution eventually turned black. After dissolving the dopant $Fe(ClO_4)_2$ in two milliliters of distilled water, it was added dropwise within the solution of PPy + Ag NPs + $FeCl_3$. At a temperature between 0° and 5°C, the polymerization was done for five hours while being continuously stirred. For twenty-four hours, this mixture was left to settle. The product had been filtrated at low pressure, rinsed with purified water till the filtrate was colorless and vacuum-dried at room temperature until its weight remained constant. When PPy is created by oxidation with the presence of $FeCl_3$, the entire reaction can be represented by the stoichiometric equation that follows. Cl^{-} anions are used to dope the polymer.

$$nC_4H_5N + (2+y)nFeCl_3 \rightarrow \left[(C_4H_3N)_n^{y} + nyCl^{-}\right] + (2+y)nFeCl_2 + 2nHCl$$

2.3 Electrical Conductivity

The powders of these samples were first crushed to a fine powder using an agate mortar and pestle. 100 milligrams of the powder was taken in to die which is 10mm in diameter. The press is capable of producing maximum pressure upto 15 tons. A pressure gauge for indication of pressure is provided. Press the prepared die into the pellet press. Pump the press under a pressure of 7 tons and let pellet sit at that pressure for a minute or two. Then loosen the front knob to release the pressure and lower the platform. Remove the die containing your pellet and the piston. The pellets made using pelletize of 10 mm diameter under a pressure of 7 tons. After applying conductive silver pastes to the pellets and vacuum-drying them, an electrical measurement was made. Two probe approaches were utillized to determine the electrical conductivity between 303 and 343 K. In our lab, we specially made the equipment for measuring conductivity using two probes. The following formula was utilized to measure electrical conductivity:

$$\sigma = \frac{I}{V} \times \frac{t}{A} \tag{1}$$

Where σ = conductivity; t = thickness; I / V = slope of I–V plot and A = area

2.4 Gas sensor setup

A layer of PPy was applied to an Inter Digitated Electrode (IDE) to create the sensor. Five sets of copper tracks were screen-printed on an epoxy substrate of glass to create the IDE. A Copper track's width and the separation of the two tracks which followed one another were both one millimetre. The overall dimensions of the device were 30 millimeters by 20 millimetres. The casting solution was made by dissolving the PPy powder in M-cresol and stirring it for a full day. Films were then created by brush-coating the paste over IDE epoxy glass substrates. After being vacuum-dried, films were used to test their gas sensing capabilities. Figure 1 displays the schematic of a manufactured gas sensor to powder samples.

A specially made gas chamber was utilized to measure the gas response. The gas chamber was equipped with the IDE sensor. To achieve the required gas concentration inside the chamber, a syringe was used to inject a measured amount of gas. A 4-digit digital multimeter with scientific programming was used to measure the resistance. To record sensor recovery, the sensor had been exposed to air after reaching a steady state. To do this, the chamber's V_1 and V_2 valves were opened simultaneously. Meanwhile, the hoover pump had been turned on. While valve V_2 permitted the gas to leave the chamber, valve V_1 permitted fresh air to enter. The degassing process was accelerated by the vacuum pump. Every gas sensitivity test was carried out at room temperature.

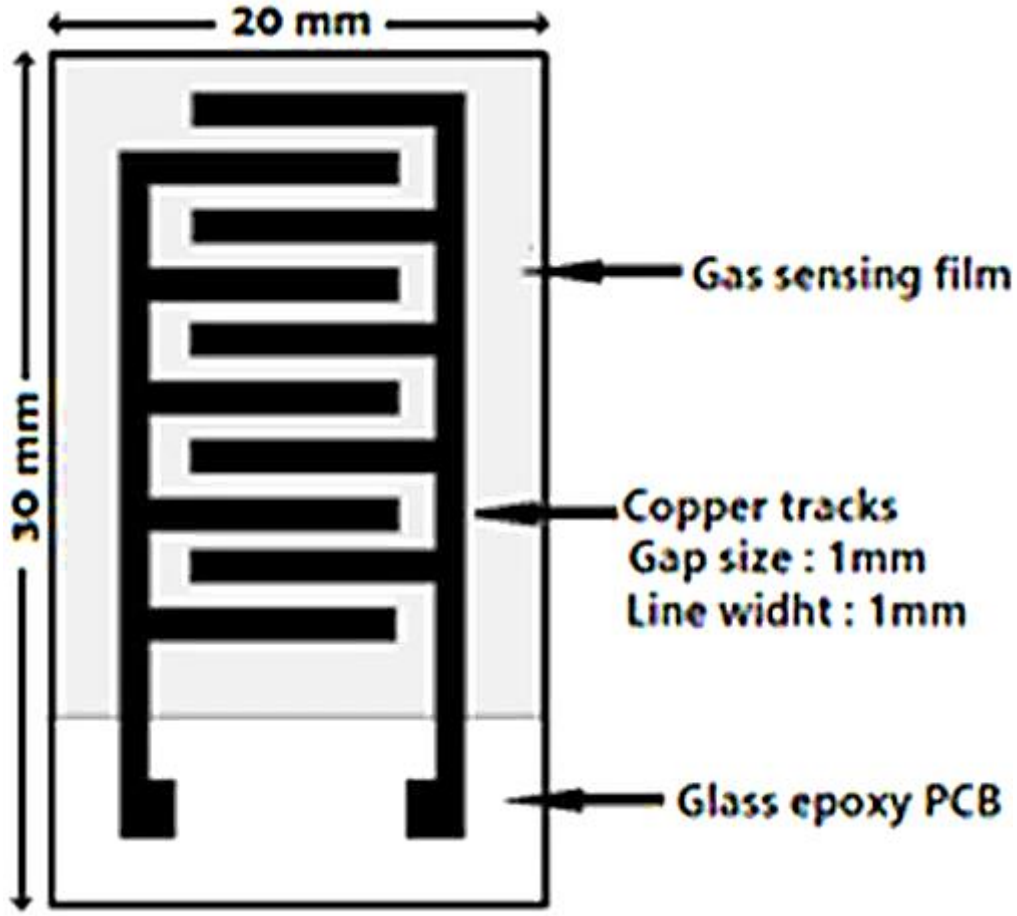

Fig 1. Structure of fabricated gas sensor

3 Results and Discussion

3.1 Scanning Electron Microscopy (SEM) and Transmission electron microscopy (TEM)

SEM images of PPy, PPy-Fe$(ClO_4)_2$, PPy-Fe$(ClO_4)_2$-Ag nanocomposite are shown in Figures 2(A), 2(B) and 2(C). A cauliflower-like morphology made up of globular grains was visible in every image. All of these typically exhibit globular morphology between 180 and 300 nm, and it looks as though the globules are growing continuously on top of each other. Because of its uniform distribution and densely packed structure, the PPy-Fe$(ClO_4)_2$-Ag nanocomposite having a high number of inter-junction forms on its surface. The gas sensing functionality is enhanced by these junctions because they permit a substantial amount of majority carriers of charge to flow across the composite as the target gas comes into contact. The composite material may function better to gas-sensitive applications because adding of Ag nanoparticles along with dopant enhances the number of sites for adsorption in the material. The TEM pictures of the PPy-Fe Fe$(ClO_4)_2$-Ag nanocomposite are displayed in Figure 2(D). The existence of Ag nanoparticles attached to the PPy matrix is confirmed by their spherical or semispherical form, and their average size is around 40 nm, which is most likely the consequence of their clustering or combining techniques.

3.2 Fourier Transform Infrared Spectroscopy (FTIR)

The FTIR spectra of the PPy-Fe$(ClO_4)_2$-Ag nanocomposite and pure PPy, obtained between 4000 and 440 cm^{-1}, are shown in Figure 3. N–H along with C–H bond stretching was identified as the cause of the broad peaks at 3440.81 and 3206.54 cm^{-1} [(2)]. The peak at 2927.78 cm^{-1} might be associated with the stretching vibrations of the CH of the N-methyl pyrrole unit while peak at 1691.47 cm^{-1} are associated with C=N bonds. The major band during 1627.77 as well 1539.33 cm^{-1} is caused by the vibration of the pyrrole ring [(17)]. The peak at 1465.81 corresponds to C-H out plane deformation. When compared to pure PPy and PPy-

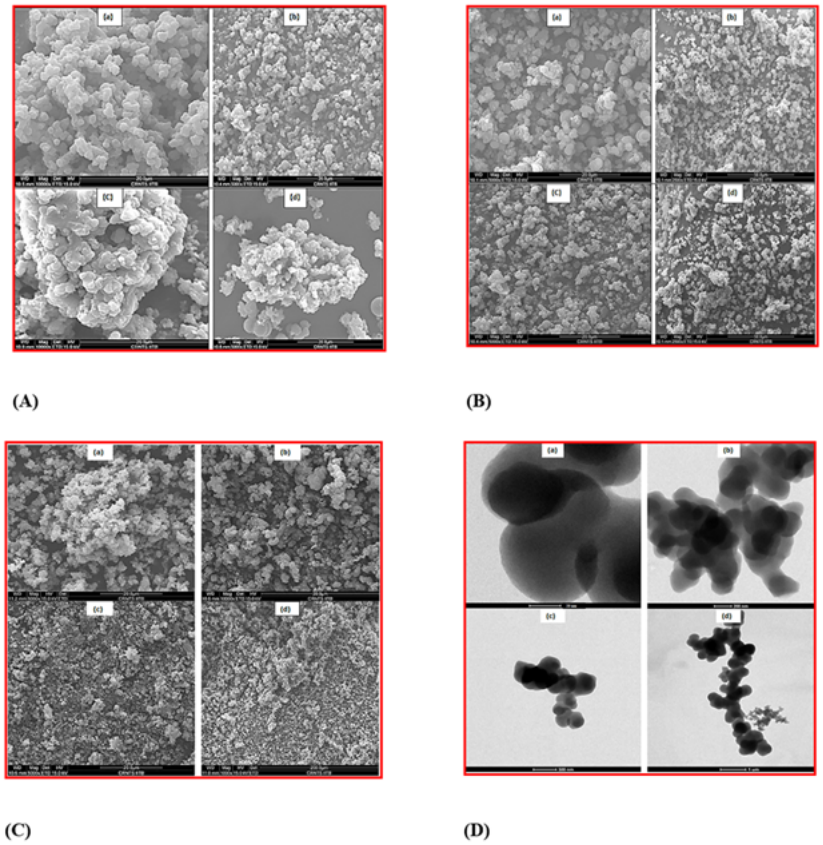

Fig 2. (A), (B), (C) are SEM images of PPy, PPy-Fe $Fe(ClO_4)_2$ and PPy-Fe $Fe(ClO_4)_2$-Ag nanocomposite and (D) is the TEM of PPy-Fe $Fe(ClO_4)_2$-Ag nanocomposite

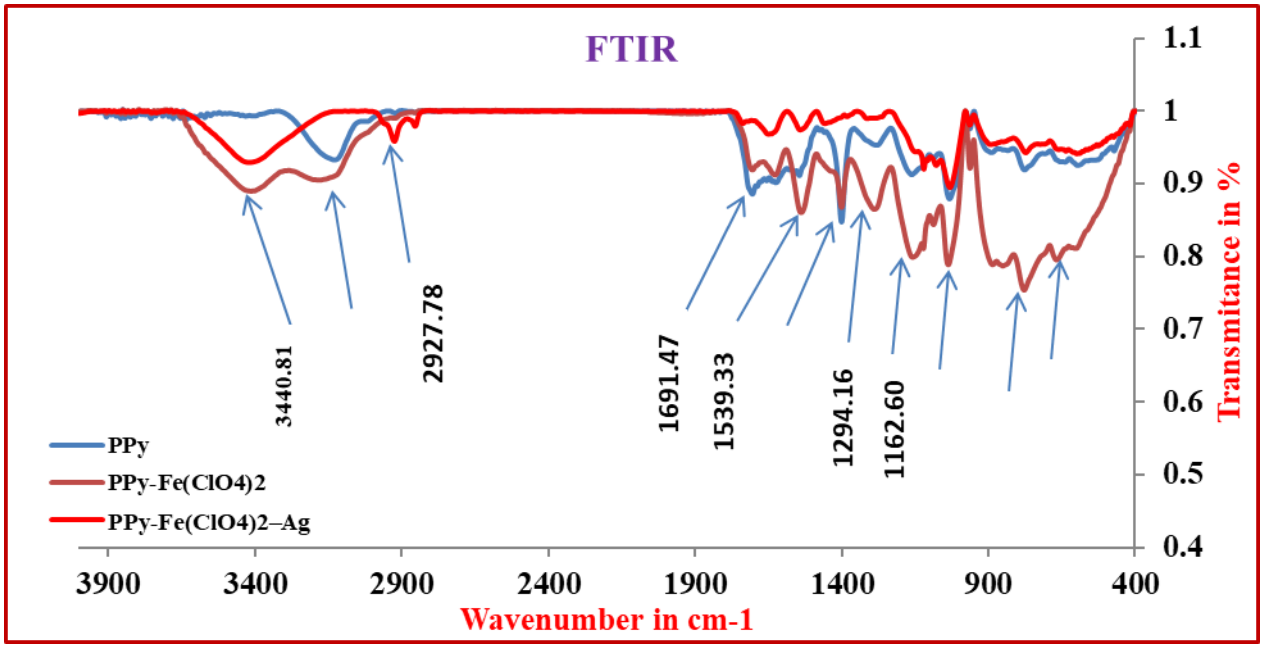

Fig 3. FTIR of Pure PPy, PPy-Fe$(ClO_4)_2$ and PPy-Fe$(ClO_4)_2$-Ag nanocomposite

$Fe(ClO_4)_2$, the spectra of PPy-$Fe(ClO_4)$-Ag exhibit slight differences in peak locations. This implies interactions between the Ag nanoparticles, the PPy matrix, and the dopant ($Fe(ClO)_2$). Electrostatic interactions between Fe^{2+} ions as well as ClO4- anions stabilize the charged structure of the PPy backbone and cause vibrational modes to shift. The band to 1041.50 cm^{-1} is associated with the =C–H in-plane vibration[8]. The band at 1294.16 cm^{-1} is caused by a N=C stretching vibration[9]. The C-H within plane bending is responsible for the peaks to 1162.60. For the FTIR spectrum of PPy, the characteristic peak that 671.92 cm^{-1} is associated with C–H wagging[8]. In PPy units, the peaks at 775.39 cm^{-1} correspond to C-H in plane deformation. All of the peaks exhibit absorption peaks that correspond to bipolaron bands, which were detected at 891.50 and 851.88 cm^{-1}, according to spectroscopic characterization of polypyrrole[18]. Bipolaron generation enhances conductivity by increasing charge density carriers. In gas sensing, bipolarons can interact with gas molecules, changing the electrical characteristics of the gas sensor. The peaks in the PPy-$Fe(ClO_4)_2$-Ag nanocomposite were shifted to a higher wavenumber than those of PPy, according to the spectra. The compound that results from the combination of silver and PPy may be the reason for this[18]. It was discovered that each peak nearly matched the values documented in the literature.

3.3 UV-Visible spectroscopy (UV-Vis)

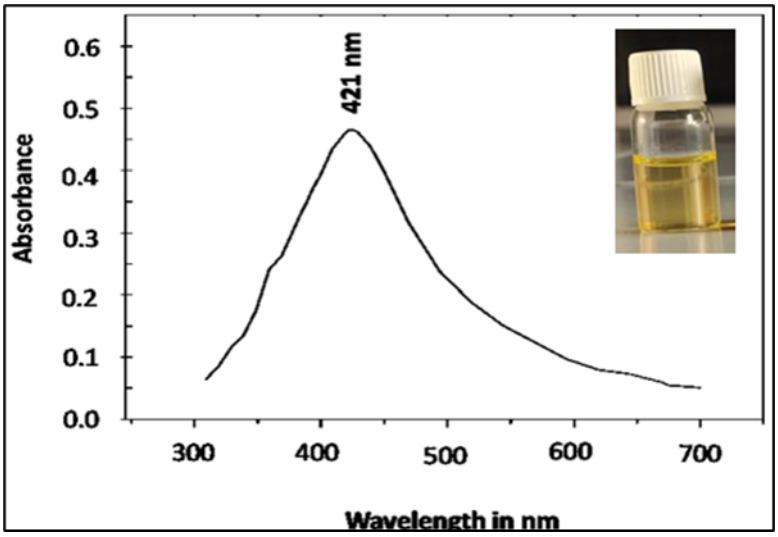

Fig 4. UV-Vis of Ag nanoparticle

Figure 4 displays UV-visible spectra for Ag nanoparticle solutions. Trisodium citrate combines the functions of a reductant as well as a stabilizer in the Turkevich method of creating silver colloids[15]. When Ag nanoparticles (Ag NPs) were formed, the color of the Ag colloidal solution, which was composed of $AgNO_3$, changed from colorless to golden yellow. The distinctive golden yellow color of colloidal silver is caused by a collective oscillation in the electron flow from the metal surface when excited by specific wavelengths of light. Surface Plasmon resonance is the term used to describe this phenomenon. The broad surface Plasmon absorbed peak at about 421 nm is observed, which validates the synthesis of Ag NPs.

3.4 X-ray Diffraction (XRD)

Figures 5(A), 5(B) and 5(C) displays the X-ray diffraction pattern for the PPy, PPy-$Fe(ClO_4)_2$, PPy-$Fe(ClO_4)_2$-Ag nanocomposite. There is a broad peak seen in the $20^\circ < 2\theta < 30^\circ$ region. The broad peak denotes short-range PPy arrangement chains and is typical of an amorphous nature[19]. As seen in Figures 5(A) to 5(C), doping results in a shift of roughly 1° in peak values towards the higher angle. This implies that the interplanar spacing decreases with the addition of dopants. The bonds might overlap more, the chains would become closer together, and the dopant interaction would be stronger as a result. Dopants increase electrical conductivity by causing the π-bonds to overlap more, which brings the polymer chains nearer together. The positively charged configuration of doped PPy interacts with the perchlorate (ClO_4^-) ions introduced by $Fe(ClO_4)_2$. These interactions might make it possible for the polymer chains to align more regularly, which would improve the crystalline regions. In Figure 5(C) the peaks at 2θ = 32.40, 46.180, 67. 440, and 77.700, respectively, the face centred cubic (FCC) phase for PPy-silver nanocomposites was found to display all of its typical peaks (1 1 1), (2 0 0), (2 2 0), and (3 1 1), which correspond to

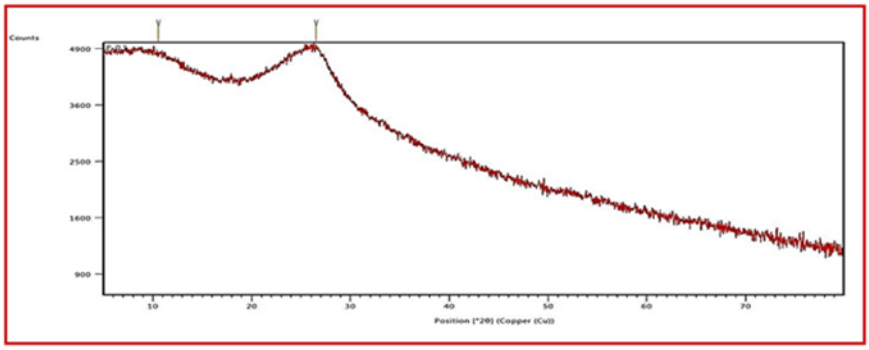

(A): XRD pattern of PPy

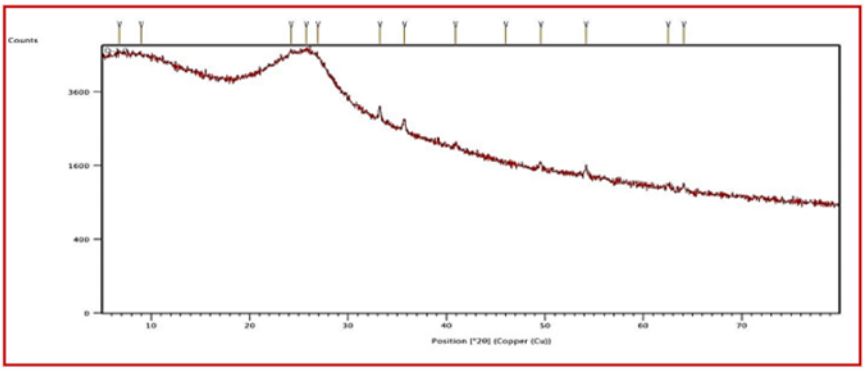

(B): XRD pattern of PPy-Fe(ClO$_4$)$_2$

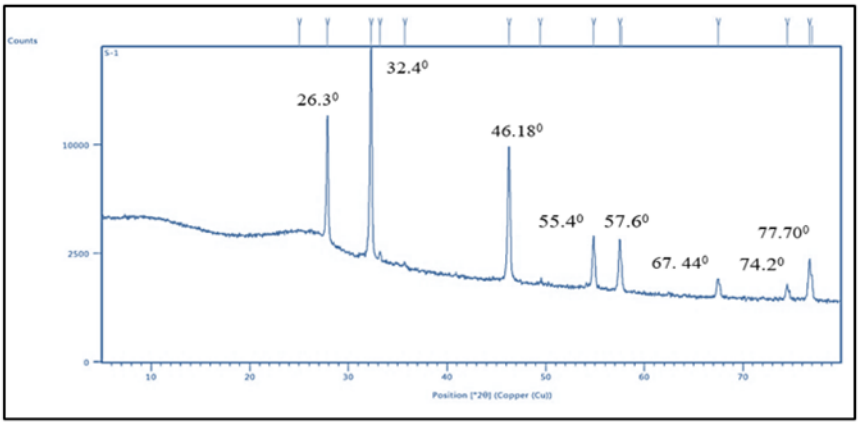

(C): XRD pattern of PPy- Fe(ClO$_4$)$_2$-Ag nanocomposite

Fig 5. X-ray diffraction pattern for the PPy, PPy-Fe(ClO$_4$)$_2$, PPy- PPy-Fe(ClO$_4$)$_2$-Ag nanocomposite

the values that were reported (JCPDS file no. 04-0783). This gives black powder containing metallic Ag[20]. Three more peaks shown in the XRD spectra at 55.40, 57.60, and 74.20. AgNO3, which is the cause of these peaks, might not have been eliminated and can be exist small amounts within the sample[19].

3.5 Thermogravimetric analysis (TGA)

Figure 6 shows the TGA curve for the PPy-Fe$(ClO_4)_2$-Ag nanocomposite, which shows three stages in weight loss. The beginning phase of weight loss, which results from the evolution of water, occurs between 25 and 130°C and is roughly 10% weight loss. Because oligomer molecules break down before 190 °C, there is a slight weight loss. The second phase of weight loss is caused by a decrease in surfactant dopant, which takes place during 190 to 380 °C. The thermal breakdown of PPy into various chemical forms is the reason for the third phase of weight loss, which occurs between 380 and 625 °C and accounts for roughly 34% of its total weight loss. Because the nanoparticles and also the polymeric chain have more intermolecular interaction, the nanocomposite has a higher thermal stability. At higher temperatures, this material is useful for gas sensing applications.

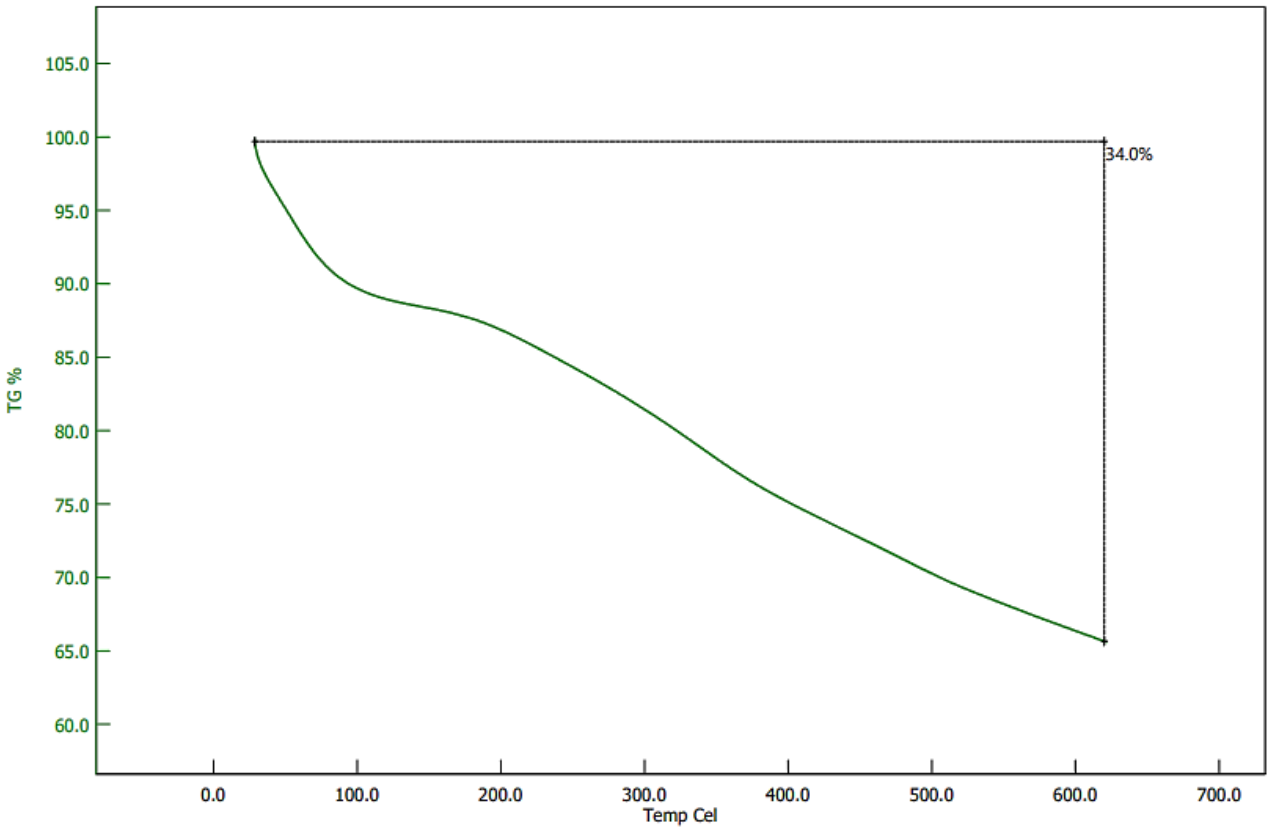

Fig 6. TGA of PPy-Fe$(ClO_4)_2$-Ag nanocomposite

3.6 DC electrical conductivity

The I-V characteristic for PPy-FeClO_4-Ag nanocomposite material was used to calculate its electrical conductivity. The I-V properties for the PPy-Fe$(ClO_4)_2$-Ag nanocomposite material at various temperatures, ranging from ambient (303 K) to 343 K, are illustrated in Figure 7. The ohmic nature of a sample, which is crucial for sensor applications as it guarantees linear as well as stable electrical performance, is evident from the curves' steady increase in current with voltage. For accurate and dependable sensor operation, this linear property is required. Ohmic contacts are essential for a variety of sensing applications because of their stability, which also adds to sensor durability and dependability[20]. **Equation (1)** was used to calculate the electrical conductivity. In comparison to PPy samples, which had an electrical conductivity of about 10^{-4}S/cm as reported by Dave et al.[9], Verma et al.[21] reported a room temperature electrical conductivity of $4.9 \times 10^{-2}\Omega^{-1}m^{-1}$ for PPy@Ag

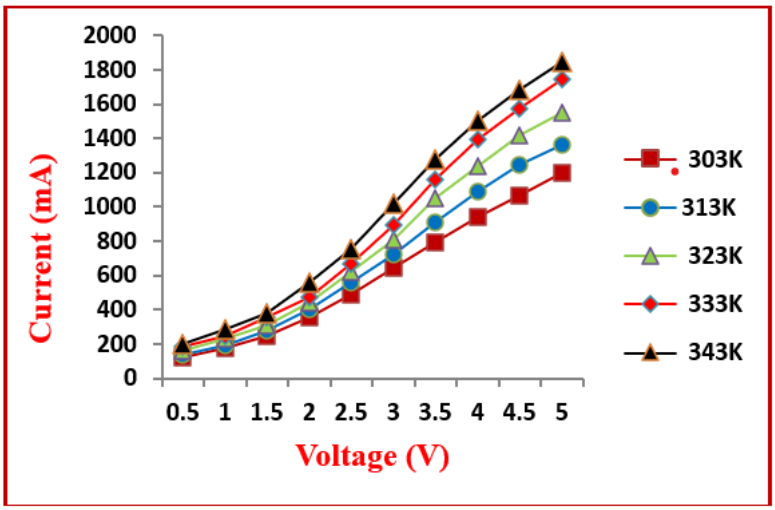

Fig 7. Current vs. voltage (I-V) characteristic of PPy-Fe$(ClO_4)_2$-Ag nanocomposite

nanocomposites, while Abdeltwab et al.[22] demonstrated that the incorporation of PPy-Ag into a PET matrix improved the composite's conductivity to $2.4 \times 10^{-6} S \cdot cm^{-1}$. Sood et al.[17] synthesized polypyrrole using $FeCl_3$ as an oxidant and achieved a conductivity of $2.22 \times 10^{-4} S \cdot cm^{-1}$, which was higher than that of APS-based PPy. In comparison, the PPy-Fe$(ClO_4)_2$-Ag nanocomposite developed in the present study exhibited a significantly higher electrical conductivity, ranging from 5.80×10^{-2} to $7.98 \times 10^{-2} S \cdot cm^{-1}$, highlighting the synergistic effect of Fe$(ClO_4)_2$ doping and silver nanoparticle incorporation on enhancing the electrical performance of polypyrrole. It appears that electronic tunnelling via the Ag NPs is responsible for the increase in conductivity[23]. This enhanced electrical conductivity at room temperature is necessary for the manufacturing of sensors[23],[24].

3.7 Gas sensing performance

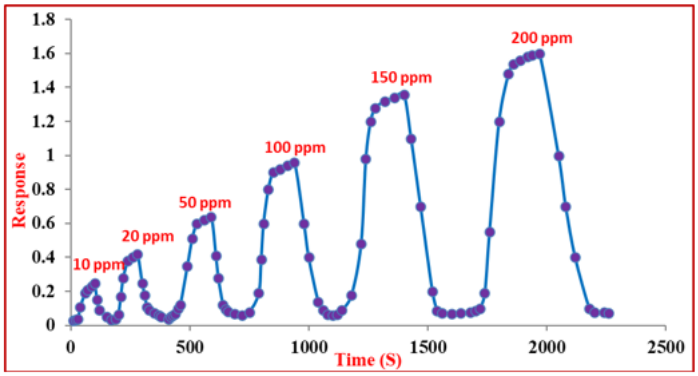

Fig 8. Sensor response for different H_2S concentrations

Figure 8 showed the response against time plots for various H_2S gas concentrations. The following formula is used to determine response factor (R).

$$R = \frac{R_g - R_a}{R_a} \tag{2}$$

Where R_g and R_a represent the gas sensor's resistances in the H_2S gas and air, respectively.

When the H_2S gas concentration was 10 ppm, 20 ppm, 50 ppm, 100 ppm, 150 ppm, and 200 ppm, the PPy-Fe$(ClO_4)_2$-Ag nanocomposite's response was 0.25, 0.42, 0.64, 0.96, 1.36, and 1.60, respectively. It was discovered that gas responses rose steadily as gas concentration rose up to 500 ppm. The linear response for H_2S gas in ranges of 10 to 200 ppm suggests that the sensor can be used to track levels of to H_2S gas over this range. The response of the PPy-Fe$(ClO_4)_2$-Ag nanocomposite to different H_2S gas concentrations, ranging from 10 ppm to 200 ppm, is shown in Figure 9. It was observed that the gas value of response increased gradually as the gas concentration raised up to 200 ppm. The sensor remains unsaturated even when the H_2S gas concentration is 200 parts per million.

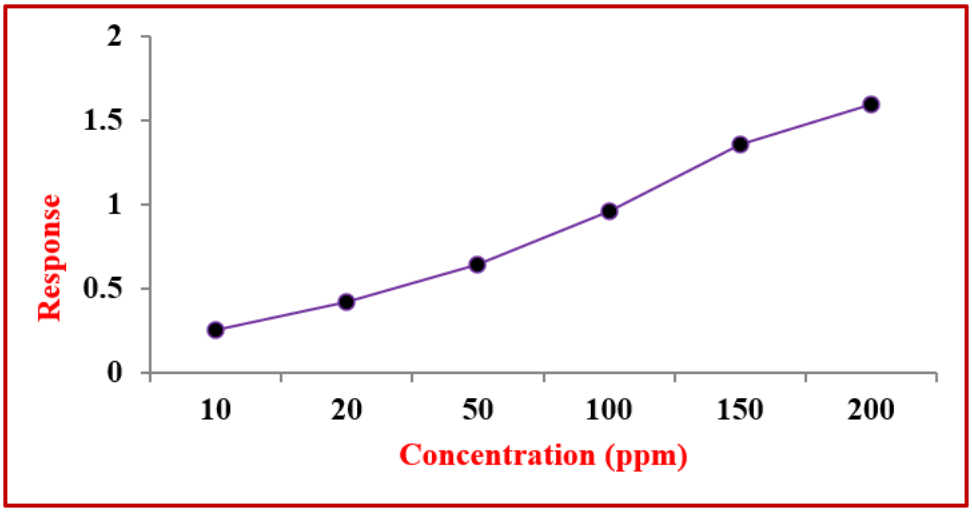

Fig 9. Response of the sensor to varying H_2S gas concentrations

Garg et al. proposed the redox reaction structure to explain the PPy's H_2S sensing mechanism. Whenever the PPy-Fe$(ClO_4)_2$-Ag nanocomposite sensor had been exposed to H_2S gas, the protonated PPy layer became doped with H^+ ions. Protons are transferred from H_2S to PPy through the redox reaction, which is linked to the fundamental sensing mechanism. The redox reaction in detail is provided as,

$$PPyH^+ + H_2S \leftrightarrow PPyH^+ \cdot H_2S \tag{3}$$

$$PPyH^+ \cdot H_2S \rightarrow PPyH^+ + H_2S + H_3O^+ \tag{4}$$

The redox reaction that takes place between the PPy and H_2S raises PPy's doping level. It was found that this led to a decline in base resistance. A schematic representation of the fundamental gas sensing principle related to PPy is given in Figure 10.

Conductivity, one of a gas sensor's primary physical properties, varies depending on how gas interacts with the sensor material on its surface. These interactions may lead to the expansion of the conducting layers, which could impact the electrical resistance along with sensing ability. Moreover, nanoscale particles have both chemical and physical characteristics[8]. The surface volume ratio and specific surface area both increase quickly as the material's size decreases. Electron and hole flow in the materials is also affected by the size and shape of the nanoparticles of semiconductors[25].

The composite's repetitive response to periodic contact with H_2S gas at 100 ppm is illustrated in Figure 11. This shows the sensor's periodic behavior when the gas flows in (absorbed) and out (desorbed). The sensor was observed to have good repeatability, meaning that it can be used frequently for detecting H_2S gas at a room temperature.

The response time for the gas sensor became the time required to detect 90% for the greatest resistance change following exposure to H_2S gas. Recovery time was defined as the amount of time needed by the sensor to restore 90% of its initial resistance. Figures 12 (A) and 12(B) shows the PPy-Fe$(ClO_4)_2$-Ag nanocomposite sensor's response and recovery time for various H_2S gas concentrations. As the H_2S concentration rose from 10 ppm to 200 ppm, it was noticed that the response time raised from 80 s to 210 s. The microstructural analysis suggests that the increase in response time with increasing H_2S concentration may be due to the large number of available sites within the nanocomposite to gas adsorption. The recovery time

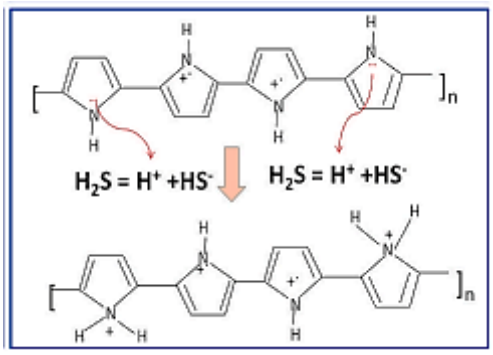

Fig 10. Gas sensing mechanism of PPy

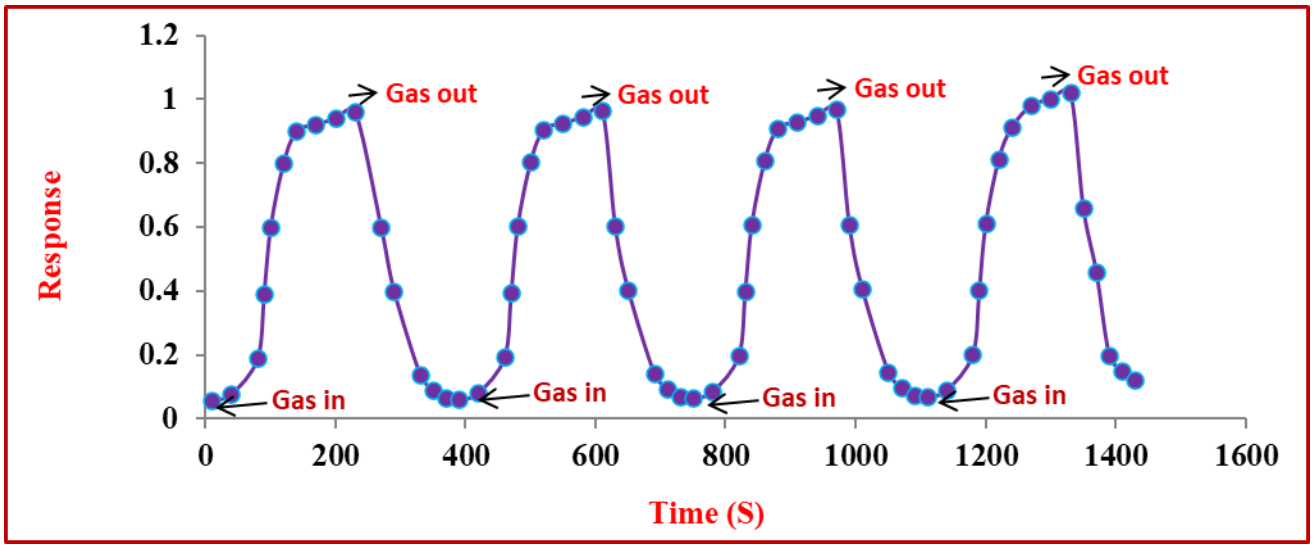

Fig 11. Repeatability response of sensor upto 100 ppm for H_2S gas

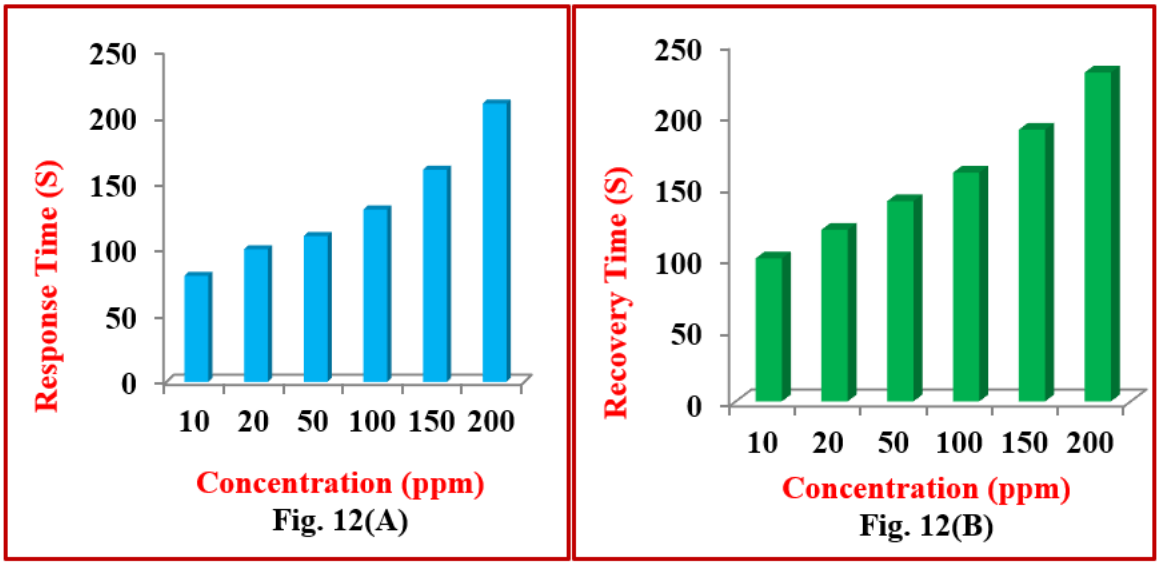

Fig 12. (A) Response and (B) recovery times of sensor for various concentrations of H_2S gas

increased from 100 s to 230 s when the H_2S concentration increased from 10 ppm to 200 ppm. The recovery time may have increased as a result of the desorption rate decreasing.

Figure 13 illustrates a composite sensor's long-term stability against H_2S gas. Over the period of 50 days, the sensor underwent testing combined with 10, 20, 50, 100, 150, and 200 ppm of gas, and its reaction was noted every 10 days. It was observed that there was slight change in the response over the 50-day period. After 50 days, the sensor maintained almost 80% of its initial value, indicating strong long-term stability. In order to improve its steady performance over time, this long-term stable sensor must be exposed to gases repeatedly without experiencing significant degradation. Improving the long-term reliability feature is essential since slight changes in reaction are seen over time.

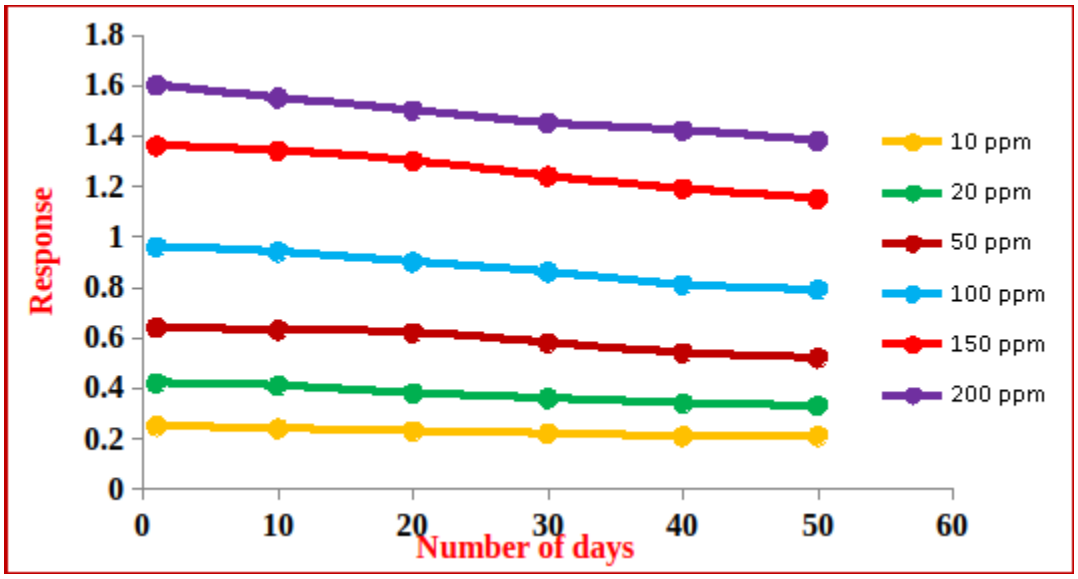

Fig 13. The long-term stability of sensor against H_2S gas

4 Conclusions

The PPy-Fe$(ClO_4)_2$-Ag nanocomposite was successfully synthesized via in situ chemical oxidative polymerization. SEM revealed a globular PPy morphology with an average size of 180–300 nm. FTIR and XRD confirmed the PPy structure, while FTIR, TEM, and UV-Vis spectroscopy verified Ag nanoparticle formation (average size 40 nm). XRD patterns showed amorphous PPy and crystalline Ag phases. TGA indicated improved thermal stability. Electrical conductivity ranged from 5.80 $\times$ 10^{-2} to 7.98 $\times$ 10^{-2} S/cm between 303K and 343K. The nanocomposite sensor exhibited excellent sensitivity, repeatability, fast response and recovery times for H_2S gas detection at low concentrations (10–200 ppm) with stable performance over 50 days. The enhanced gas sensing performance is attributed to Ag nanoparticle intercalation, improving surface area and charge transfer. These results highlight the potential of PPy-Fe$(ClO_4)_2$-Ag as an efficient room temperature operative H_2S gas sensor.

5 Declaration of competing interest

The authors declare that they have no known competing financial interests or personal relationships that could have appeared to influence the work reported in this paper.

6 Acknowledgement

The authors would like to express their sincere gratitude to the Department of Metallurgical Engineering and Materials Science and Sophisticated Analytical Instrument Facility (SAIF) at the Indian Institute of Technology (IIT) Bombay for providing the characterization of our samples.

References

1) More VS, Sakhare BK, Tandel RP, Padhye GG, Ghorude TN. Electric Elegance: Enhancing Cotton Fabric with Conducting Polypyrrole for Gas Sensing Applications. *Mapana Journal of Sciences*. 2024;22:59–76. https://doi.org/10.12723/mjs.67.4.
2) More VS, Patil MP, Tandel RP, Ghorude TN, Padhye GG. Study of Structural, Morphological, Electrical, and Thermal Characteristics of PPy-Fe(ClO4)2 -Au Nanocomposite and its Application in Ammonia Gas Sensing. *Indian J Sci Technol*. 2024;17:4842–4853. https://doi.org/10.17485/IJST/v17i46.3148.
3) Kroutil J, Laposa A, Povolny V, Klimsa L, Husak M. Gas Sensor with Different Morphology of PANI Layer. *Sensors*. 2023;23. https://doi.org/10.3390/s23031106.
4) More VS, Ghorude TN, Patil MP, Sakhare BK, Tandel RP, Padhye GG. Comprehensive Analysis of γ-Radiation Impact on PVA-PTh Composite Films for Enhanced Battery Functionality. *Indian J Sci Technol*. 2023;16:4349–4357. https://doi.org/10.17485/IJST/v16i46.2256.
5) Das M, Roy S. Polypyrrole and associated hybrid nanocomposites as chemiresistive gas sensors: A comprehensive review. *Mater Sci Semicond Process*. 2021;121:105332. https://doi.org/10.1016/j.mssp.2020.105332.
6) Shoeb M, Mobin M, Ahmad S, Naqvi AH. Facile synthesis of polypyrrole coated graphene Gr/Ag–Ag2O/PPy nanocomposites for a rapid and selective response towards ammonia sensing at room temperature. *Journal of Science: Advanced Materials and Devices*. 2021;6:223–233. https://doi.org/10.1016/j.jsamd.2021.02.003.
7) Franco MA, Conti PP, Andre RS, Correa DS. A review on chemiresistive ZnO gas sensors. *Sensors and Actuators Reports*. 2022;4:100100. https://doi.org/10.1016/j.snr.2022.100100.
8) Pagar SB, Ghorude TN, Nikolova MP, SenthilKannan K. Synthesis, physical, chemical, biological, mechanical and electronic studies of polypyrrole (PPy) of versatile scales for electro-mechano, pharmaceutical utilities. *Heliyon*. 2023;9:e20086. https://doi.org/10.1016/j.heliyon.2023.e20086.
9) Dave NV, Nerkar DM. The influence of the oxidant on structural and morphological properties of conductive polypyrrole. *Mater Today Proc*. 2021;45:5939–5943. https://doi.org/10.1016/j.matpr.2020.09.104.
10) Abhishek N, Verma A, Singh A, Vandana, Kumar T. Metal-conducting polymer hybrid composites: A promising platform for electrochemical sensing. *Inorg Chem Commun*. 2023;157:111334. https://doi.org/10.1016/j.inoche.2023.111334.
11) Masuda Y. Recent advances in SnO2 nanostructure based gas sensors. *Sens Actuators B Chem*. 2022;364:131876. https://doi.org/10.1016/j.snb.2022.131876.
12) Su PG, Chai XC. Room-Temperature ppb-Level H2S Gas Sensors Based on Ag Nanowire/Hollow PPy Nanotube Nanocomposites. *Chemosensors*. 2022;10:305. https://doi.org/10.3390/chemosensors10080305.
13) Liu X, Zheng W, Kumar R, Kumar M, Zhang J. Conducting polymer-based nanostructures for gas sensors. *Coord Chem Rev*. 2022;462:214517. https://doi.org/10.1016/j.ccr.2022.214517.
14) Zhang Z, Du H, Yi W, Sun Y, Zheng Y, Wu Y, et al. Investigation of Ammonia-sensing Mechanism on Polypyrrole Gas Sensor Based on Experimental and Theoretical Evidence. *Sensors and Materials*. 2021;33:1443. https://doi.org/10.18494/SAM.2021.3330.
15) Dong J, Carpinone PL, Pyrgiotakis G, Demokritou P, Moudgil BM. Synthesis of precision gold nanoparticles using Turkevich method. *KONA Powder and Particle Journal*. 2020;37:224–232. https://doi.org/10.14356/kona.2020011.
16) Nguyen KV, Trung BH, Tuan CV, Sai CD, Vu TD, Trung T, et al. Ammonia gas-sensing behavior of uniform nanostructured PPy film prepared by simple-straightforward in situ chemical vapor oxidation. *Open Physics*. 2023;21. https://doi.org/10.1515/phys-2022-0232.
17) Sood Y, Mudila H, Katoch A, Lokhande PE, Kumar D, Sharma A, et al. Eminence of oxidants on structural–electrical property of Polypyrrole. *Journal of Materials Science: Materials in Electronics*. 2023;34. https://doi.org/10.1007/s10854-023-10834-8.
18) Kadhem SJ. Studying of Plasma- Polymerized Pyrrole at Variable Gas Flow Rates Via Plasma Jet. *Iraqi Journal of Physics*. 2021;19:44–51. https://doi.org/10.30723/ijp.v19i48.593.
19) Wu C, Xu S, Wang W. Synthesis and applications of silver nanocomposites: A review. *J Phys Conf Ser*. 2021;1948. https://doi.org/10.1088/1742-6596/1948/1/012216.
20) Berger C, Alquier D, Michaud JF. How to Accurately Determine the Ohmic Contact Properties on n-Type 4H-SiC. *Electronics (Basel)*. 2024;13:217. https://doi.org/10.3390/electronics13010217.
21) Verma A, Kumar T, Singhal R. Silver doped Polypyrrole nanocomposite-based gas sensor for enhanced ammonia gas sensing performance at room temperature. *Chemical Physics Impact*. 2024;9:100722. https://doi.org/10.1016/j.chphi.2024.100722.
22) Abdeltwab E, Al-Harbi N, Atta A, Abdelhamied MM. Influence of silver nanoparticles on the surface characteristics and electrical properties of polypyrrole/PET polymeric composite films for electronic devices. *Int J Mod Phys B*. 2025;39. https://doi.org/10.1142/S0217979225501292.
23) Sood Y, Singh K, Mudila H, Lokhande PE, Singh L, Kumar D, et al. Insights into properties, synthesis and emerging applications of polypyrrole-based composites, and future prospective: A review. *Heliyon*. 2024;10:e33643. https://doi.org/10.1016/j.heliyon.2024.e33643.
24) Sood Y, Lawaniya SD, Mudila H, Katoch A, Awasthi K, Kumar A. Ultra-high performance of PPy/MoS2 2D nanocomposites for ammonia sensing. *Sens Actuators B Chem*. 2024;417:136165. https://doi.org/10.1016/j.snb.2024.136165.
25) Nikolic MV, Milovanovic V, Vasiljevic ZZ, Stamenkovic Z. Semiconductor Gas Sensors: Materials, Technology, Design, and Application. *Sensors*. 2020;20:6694. https://doi.org/10.3390/s20226694.